Supporting information for: Intercalation Kinetics in Multiphase Layered Materials

Raymond B. Smith,[†] Edwin Khoo,[†] and Martin Z. Bazant[*,†,‡]

†*Department of Chemical Engineering, Massachusetts Institute of Technology, Cambridge, Massachusetts 02139, USA*

‡*Department of Mathematics, Massachusetts Institute of Technology, Cambridge, Massachusetts 02139, USA*

E-mail: bazant@mit.edu

Simulation Details for Examining Axial Symmetry Assumption

In the interest of keeping the 2D simulation time to a few hours, we perform the simulation up to $t = 1553$ s instead of $t = 6210$ s as in ref. S1. We impose no-flux boundary conditions on the straight edges of the sector and lithium intercalates along the arc of the sector. In Figure S1, we plot $\widetilde{c}_1$ at $t = 669$ s where axial symmetry is broken, and at $t = 1553$ s where axial symmetry is not broken. We provide plots of $\widetilde{c}_1$ against r at $\theta = 0°$ and $\theta = 0.352°$ to examine how axial symmetry is broken or not broken. In addition, we compare these $\widetilde{c}_1$ plots with those obtained from a 1D simulation in COMSOL Multiphysics using the same grid spacing of 1.43×10^{-7} m to examine how well the 1D model approximates the 2D model. This grid spacing is larger than the approximate value of the interface width in these simulations (7.1×10^{-8} m), which is a compromise on accuracy to speed up the simulations and enable a larger central angle for the 2D sector. We retain the same grid spacing in both cases in Figure S1 to focus on the comparison rather than accurate model predictions. Full movies are provided in the supplement.

In Figure S1, comparing plots (a), (c) and (e) for $t = 669$ s, we observe that axial symmetry in the $\widetilde{c}_1$ profile is broken; for instance, at the arc of the sector, $\widetilde{c}_1$ increases with increasing θ. On the other hand, comparing plots (b), (d) and (f) for $t = 1553$ s, $\widetilde{c}_1$ does not vary as a function of θ and axial symmetry is not broken. More generally, even though we initialize $\widetilde{c}_1$ and $\widetilde{c}_2$ to be 10^{-2} uniformly, we observe that axial symmetry is broken immediately, turns "less broken" as t increases, first becomes unbroken at $t = 776$ s (not shown in Figure S1, but can be seen in the full videos in the supplement), and then remains unbroken till $t = 1553$ s. Although we did not perform 2D simulations up to $t = 6210$ s as was done in ref. S1, we expect that axial symmetry remains unbroken from $t = 1553$ s to $t = 6210$ s. Comparing plots (c) and (e) with (g), the broken axial symmetry at $t = 669$ s causes some deviations between the $\widetilde{c}_1$ profiles for $\theta = 0°$, $\theta = 0.352°$ and

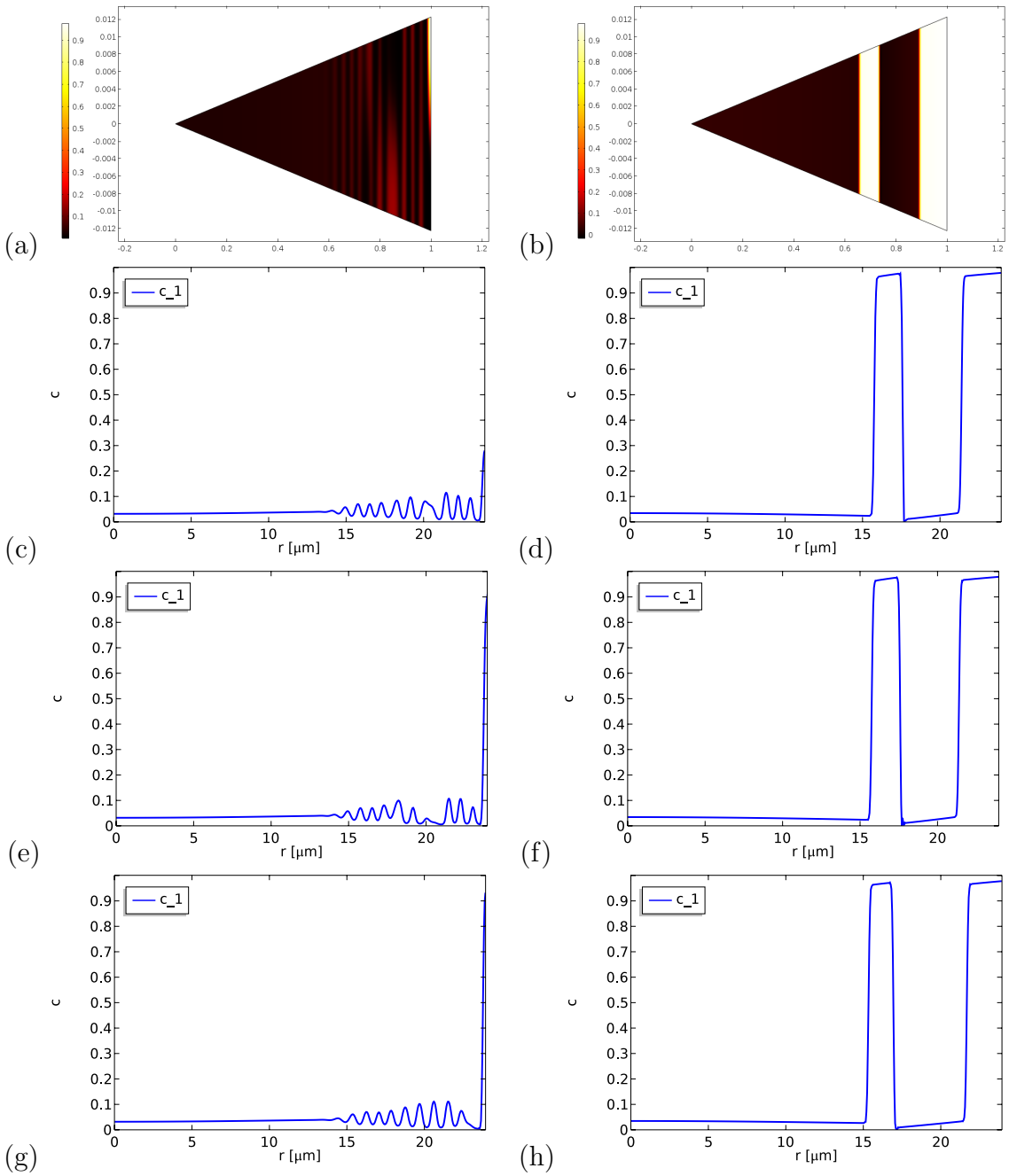

Figure S1: 2D and 1D simulations from ref. S1 performed using COMSOL Multiphysics (finite element discretization). (a) and (b) are a repeat of Figure 6 for easy comparison. Snapshots in (a), (c), (e) and (g) are taken at $t = 669$ s and those in (b), (d), (f) and (h) are taken at $t = 1553$ s. Snapshots from the 2D simulation in (c) and (d) are taken at $\theta = 0°$ and those in (e) and (f) are taken at $\theta = 0.352°$. Snapshots in (g) and (h) are taken from the 1D simulation.

the true 1D simulation. However, comparing plots (d) and (f) with (h), these $\widetilde{c}_1$ profiles agree reasonably well with each other when axial symmetry is not broken at $t = 1553$ s; this

also holds true when axial symmetry first becomes unbroken at $t = 776$ s. Crucially, the four internal domains for $\widetilde{c}_1$ in the 2D simulation are also reproduced by the 1D simulation. Therefore, the 1D simulation approximates the 2D simulation reasonably well except at early times where there are minor deviations that do not significantly affect the accuracy of the 1D simulation at later times.

Matching Diffusive Behavior in Solid Solution and Phase Separating Simulations

To approximately match the transport behavior of the two models, it is helpful to rearrange the flux expression in Eqs. 10 and 11 in terms of a chemical diffusivity, which is valid in regions where the gradient term is negligible (far from phase interfaces),

$$\mathbf{F}_i \approx -\frac{D_0}{k_\mathrm{B}T}\frac{c_i\gamma_i}{\gamma^d_{\ddagger,i}}\frac{\partial\mu_i}{\partial\widetilde{c}_i}\boldsymbol{\nabla}\widetilde{c}_i = -D_{\mathrm{chem},i}\boldsymbol{\nabla}c_i \tag{S1}$$

where

$$D_{\mathrm{chem},i} = \frac{D_0}{k_\mathrm{B}T}\frac{\widetilde{c}_i\gamma_i}{\gamma^d_{\ddagger,i}}\frac{\partial\mu_i}{\partial\widetilde{c}_i} \tag{S2}$$

$$= \frac{D_0}{k_\mathrm{B}T}\frac{\widetilde{c}_i\gamma_i}{\gamma^d_{\ddagger,i}}\left[\frac{k_\mathrm{B}T}{\widetilde{c}_i(1-\widetilde{c}_i)} - 2\Omega_a - 2\Omega_c\widetilde{c}_j(1-\widetilde{c}_j)\right]. \tag{S3}$$

Here, we are constrained on our choice for the ratio $\gamma_i/\gamma^d_{\ddagger,i} > 0$ by the second law of thermodynamics[S2], so we cannot choose it such that we have perfectly constant $D_{\mathrm{chem},i}$. We note that the choice originally proposed in Appendix A and simplified in Eq. 12 gives us[S1]

$$D_{\mathrm{chem},i} = \frac{D_0}{k_\mathrm{B}T}(k_\mathrm{B}T - 2\Omega_a\widetilde{c}_i(1-\widetilde{c}_i) - 2\Omega_c\widetilde{c}_i(1-\widetilde{c}_i)\widetilde{c}_j(1-\widetilde{c}_j)), \tag{S4}$$

$$\approx D_0 \qquad \text{far from phase interfaces.} \tag{S5}$$

Another natural choice may be to assume constant prefactor in front of the $\boldsymbol{\nabla}\mu_i$, or

$$\frac{\widetilde{c}_i\gamma_i}{\gamma^d_{\ddagger,i}} = 1, \tag{S6}$$

leading to

$$D_{\text{chem},i} = \frac{D_0}{k_\text{B}T}\left[\frac{k_\text{B}T}{\widetilde{c}_i(1-\widetilde{c}_i)} - 2\Omega_a - 2\Omega_c\widetilde{c}_j(1-\widetilde{c}_j)\right] \tag{S7}$$

which has been used in a similar model[S3] and has diverging chemical diffusivity near full and empty states. We also find this model specified by Eq. S6 to match porous electrode data in our companion paper in which the particle models are describing effective properties of secondary (polycrystalline) graphite particles[S4]. However, to retain the most similar behavior of chemical diffusivity between the solid solution and phase separating models, we focus here on the model proposed in Eq. 12.

Diffusional Chemical Potential for Single-Variable Model Reduction

In the reduced thermodynamic model for lithium intercalation in graphite, the function describing the diffusional chemical potential as a function of a single total filling fraction variable is given by

$$\frac{\mu_\text{op}(\widetilde{c})}{k_\text{B}T_\text{ref}} = 0.18 + \widetilde{\mu}_A(\widetilde{c}) + \widetilde{\mu}_B(\widetilde{c}) + \widetilde{\mu}_C(\widetilde{c}) + \widetilde{\mu}_D(\widetilde{c}) + \widetilde{\mu}_E(\widetilde{c}) - \frac{\kappa}{c_\text{ref}k_\text{B}T_\text{ref}}\nabla^2\widetilde{c} \tag{S8}$$

where

$$\widetilde{\mu}_A(\widetilde{c}) = \Bigg(-40\exp\Bigg(-\frac{\widetilde{c}}{0.015}\Bigg) + 0.75\Bigg(\tanh\Bigg(\frac{\widetilde{c}-0.17}{0.02}\Bigg) - 1\Bigg) + \Bigg(\tanh\Bigg(\frac{\widetilde{c}-0.22}{0.04}\Bigg) - 1\Bigg)\Bigg) S_D(\widetilde{c}, 0.35, 0.05) \tag{S9}$$

$$\widetilde{\mu}_B(\widetilde{c}) = -\frac{0.05}{\widetilde{c}^{0.85}} \tag{S10}$$

$$\widetilde{\mu}_C(\widetilde{c}) = 10 S_U(\widetilde{c}, 1, 0.045) \tag{S11}$$

$$\widetilde{\mu}_D(\widetilde{c}) = 6.12\big(0.4 - \widetilde{c}^{0.98}\big) S_D(\widetilde{c}, 0.49, 0.045) S_U(\widetilde{c}, 0.35, 0.05) \tag{S12}$$

$$\widetilde{\mu}_E(\widetilde{c}) = (1.36(0.74 - \widetilde{c}) + 1.26) S_U(\widetilde{c}, 0.5, 0.02) \tag{S13}$$

and step up and step down functions respectively defined by

$$S_U(x, x_c, \delta) = 0.5\Bigg(\tanh\Bigg(\frac{x - x_c}{\delta}\Bigg) + 1\Bigg) \tag{S14}$$

$$S_D(x, x_c, \delta) = 0.5\Bigg(-\tanh\Bigg(\frac{x - x_c}{\delta}\Bigg) + 1\Bigg). \tag{S15}$$

The homogeneous free energy can be computed from an integral of the homogeneous contribution to the diffusional chemical potential.

References

(S1) Guo, Y.; Smith, R. B.; Yu, Z.; Efetov, D. K.; Wang, J.; Kim, P.; Bazant, M. Z.; Brus, L. E. Li Intercalation into Graphite: Direct Optical Imaging and Cahn–Hilliard Reaction Dynamics. *The Journal of Physical Chemistry Letters* **2016**, *7*, 2151–2156.

(S2) Groot, S. R. D.; Mazur, P. *Non-Equilibrium Thermodynamics*; Interscience Publishers, Inc.: New York, 1962.

(S3) Hawrylak, P.; Subbaswamy, K. R. Kinetic Model of Stage Transformation and Intercalation in Graphite. *Physical Review Letters* **1984**, *53*, 2098.

(S4) Thomas-Alyea, K. E.; Jung, C.; Smith, R. B.; Bazant, M. Z. In Situ Observation and Mathematical Modeling of Lithium Distribution within Graphite. *Journal of The Electrochemical Society* **2017**, *164*, E3063–E3072.